Bagassa guianensis ethanol extract used as sustainable eco-friendly inhibitor for zinc corrosion in 3% NaCl: Electrochemical and XPS studies

Mounim Lebrini, Fabienne Suedile, Paule Salvin, Christophe Roos, Abdelkader Zarrouk, Charafeddine Jama, Fouad Bentiss

Bagassa guianensis ethanol extract used as sustainable eco-friendly inhibitor for zinc corrosion in 3% NaCl: Electrochemical and XPS studies

M. Lebrini [a], F. Suedile [a], P. Salvin [a], C. Roos [a], A. Zarrouk [b,*], C. Jama [c], F. Bentiss [c,d,*],

[a] *Laboratoire Matériaux et Molécules en Milieux Agressifs; EA 7526, Département Scientifique Interfacultaire, Campus Universitaire de Schoelcher B.P. 7209 F - 97275 Schoelcher, Martinique, France*
[b] *Laboratory of Materials, Nanotechnology and Environment, Faculty of Sciences, Mohammed V University, Av. Ibn Battouta, Po Box 1014 Agdal-Rabat, Morocco*
[c] *Univ. Lille, CNRS, INRAE, Centrale Lille, UMR 8207, - UMET - Unité Matériaux et Transformations, F-59000 Lille, France*
[d] *Laboratory of Catalysis and Corrosion of Materials, Faculty of Sciences, Chouaib Doukkali University, Po Box 20, M-24000 El Jadida, Morocco*

** Corresponding authors.*
E-mail address: azarrouk@gmail.com (AZ)
fbentiss@gmail.com (FB)

Graphical abstract

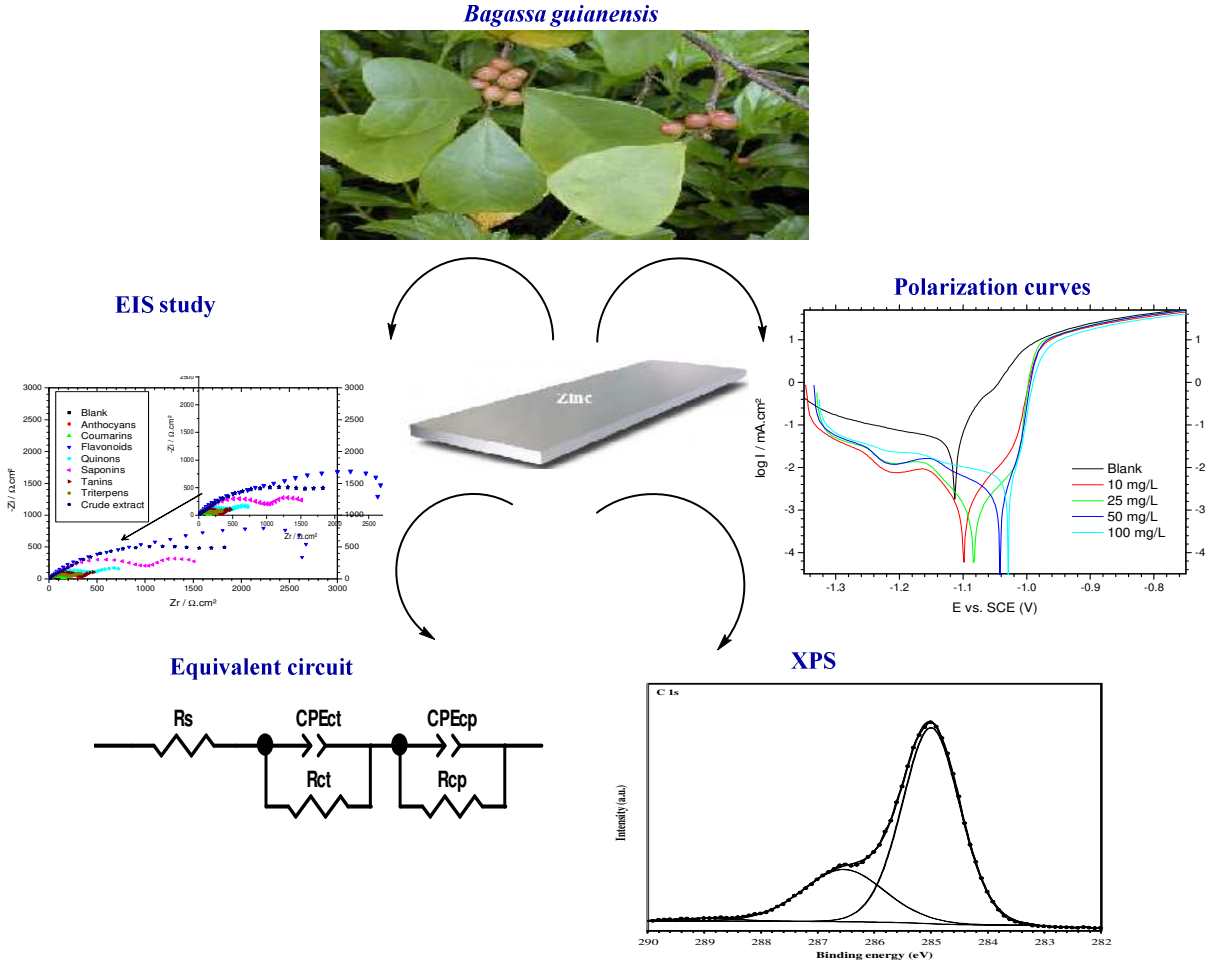

Highlights

- The plant extract of *Bagassa guianensis* is good eco-friendly corrosion inhibitor for zinc in 3% NaCl solution.
- *EEBGP* acts as mixed-type inhibitor.
- Flavonoid family dominates the inhibitory activity in the crude extract.
- XPS analyses were used to explain the *EEBGP* mechanism of zinc corrosion inhibition.

ABSTRACT

In view of the huge advantages of green corrosion inhibitors and in order to solve the problem of environmental pollution in the process of cleaning the zinc metal, this study is the evaluation of *Bagassa guianensis* extract on the corrosion behaviour of zinc in chloride medium (3%) was realised using electrochemical techniques (polarisation and AC impedance). This study demonstrated that the plant extract of *Bagassa guianensis* is a real as sustainable and green inhibitor for zinc corrosion in 3% NaCl with an inhibition efficiency of about 97% at 100 ppm. The electrochemical reactions were both impacted by the existence of the green inhibitor on the basis of the polarization curves and a change towards the positive potentials was measured in the presence of the extract in 3% NaCl. A CPE_{α}, Q determined by fit and graphical methods plotted by synthetic data, was utilized. In order to determine the chemical compounds mainly responsible for the corrosion inhibition of the extract, electrochemical studies were carried out on each family contained in the plant extract. To comprehend the adsorption mechanism of total extract and flavonoids extract for zinc in the saline solution, XPS technique was accomplished. The obtained results indicated the establishment of protective film inclosing the *Bagassa guianensis* extract and the flavonoids compounds. The mechanism of corrosion protection of *Bagassa guianensis* extract was discussed with PDP, EIS, isothermal adsorption model and XPS technique.

Keywords: *Bagassa guianensis*, Green corrosion inhibitor; Zinc protection; Electrochemical studies; XPS.

1. Introduction

Zinc is commonly used in numerous industries and fields. Its most important commercial application is in the corrosion protection of steel, for which it is extensively employed to coat or galvanize ferrous metallic products. However, it ranks fourth among the metals in worldwide production and consumption [1]. The most important application of zinc is coating for steel corrosion protection. In addition, zinc is an important component in paints, cosmetics, pharmaceuticals, storage batteries, electrical equipment and an endless list of other capital applications [2]. Investigation into the corrosion tendencies of zinc can lead to important applications in production and economics. The use of inhibitors is one of the most practical methods which can be used to protect zinc from corrosion, particularly in acidic media [3,4]. Organic inhibitors with electron donating groups such as nitrogen, sulphur and oxygen often play an important role in zinc corrosion prevention [5-10]. However, these molecules can be expensive, toxic and not easy to obtain at the industrial scale. Thus, development of new, inexpensive and safe inhibitors for corrosion protection is required. Plant extracts have become important as nontoxic, biodegradable, eco-friendly, readily available and extensible source of corrosion inhibitors. For example, the use of the plant extract of *Mansoa alliacea* as efficient corrosion inhibitor for zinc in sodium chloride solution was previously described [11]. El-Etre et al. have tested the aqueous extract of the leaves of henna (*lawsonia*) as corrosion inhibitor of zinc in neutral solutions, using the polarization technique [12]. They found that the investigated extract acts as a good corrosion inhibitor in the tested media. Recently, Nady tested tricine (N (tri (hydroxymethyl) methyl) glycine) as an eco-friendly green inhibitor for corrosion control of zinc electrode in 0.5 M NaCl corrosive solution using potentiodynamic polarization and electrochemical impedance spectroscopy (EIS) techniques [13]. A corrosion inhibition efficiency of about 90.4% was recorded in the presence of 10 mM of tricinine in 0.5 M NaCl solution. The protection of the zinc against the corrosion in 3% NaCl using ethanol extract of *Mansoa alliacea*

in order to develop a natural extract in a green solvent was reported [11]. High inhibition corrosion performances were obtained using such green inhibitor.

This study aims to gain some insight into the corrosion of zinc in 3% NaCl in the presence of ethanol extract from *Bagassa guianensis* plant (*EEBGP*) as an eco-friendly corrosion inhibitor. *Bagassa guianensis* is a shared tree original from the north of South America. It contains sterols and flavonoids [14,15]. The objective of this work is to evaluate the inhibitive influence of natural extract from *Bagassa guianensis* plant (*EEBGP*) on zinc corrosion in 3% NaCl by electrochemical techniques (Polarization and AC impedance). X-ray photoelectron spectroscopy (XPS) and phytochemistry analyses have been applied in order to establish the adsorption of molecules from the total extract (*EEBGP*) such as flavonoids onto the zinc surface.

2. Experimental

The plant extract is obtained by two methods of extraction using water/ethanol as cheap and green solvent according to a previous study [13]. Some phytochemical tests were realized to qualify and quantify the chemical constituents of the plant extract according to an earlier experimental process [16,17]. As an example of these tests, Wagner and Dragendroff tests for the existence of alkaloids and Wilstater tests for flavonoids and leucoanthocyanidin. Separation of the components from the total extract was carried out by liquid chromatography (UHPLC-DAD Ultimate 3000, Thermo Scientific).

Electrochemical experiments were carried out by means of impedance equipment (VMP3, Bio-Logic) and controlled with graphing and analysing impedance software, version EC-Lab V10.20. The working surface was subsequently ground with 1200 grit grinding papers, cleaned by distilled water and ethanol. The tested corrosive media is a 3% NaCl media at 25 °C. The preparation of solutions and the corrosion tests (polarization curves and AC impedance measurements) were conducted according to a previously described experimental procedure [13].

X-ray photoelectron spectroscopy (XPS) spectra were registered using XPS KRATOS, AXIS UltraDLD spectrometer Thermo Scientific K-Alpha XPS system. The XPS experiment and data treatment were made according to the same procedures previously described [18]. In addition to this procedure, quantification took into account a non-linear Shirley background subtraction [19].

3. Results and discussion

3.1. Preparation of ethanol extract

Reflux and ultrasound extractions, using water/ethanol (30/70) as cheap and green solvent, were employed to prepare the inhibitor extract. The analysis of the infrared spectrum (Fig. 1) displays practically identical bands of the extract with a small difference in the peak intensity. These results clearly show the presence of identical functional groups with a difference in the concentration of molecules in the two extracts obtained by the both methods. It should be noted that the high yield was obtained under reflux.

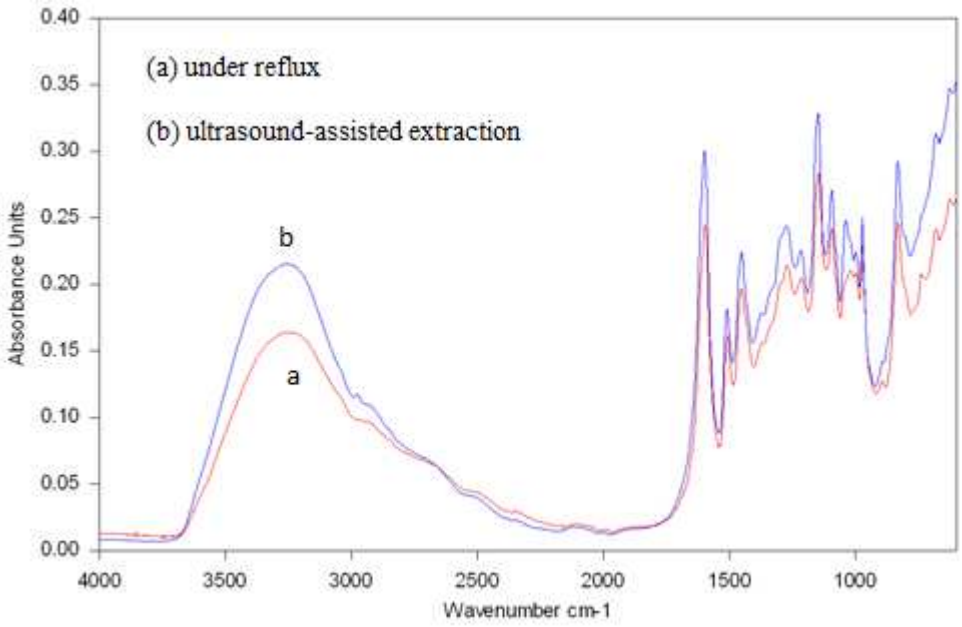

Fig. 1. Infrared spectrum of *EEBGP* obtained under reflux and ultrasound-assisted extraction.

3.2. Polarization results

Polarization curves of the zinc in 3% NaCl, in the presence of *EEBGP* obtained by the two methods of extraction, are shown in Figs. 2 and 3. These figures show that all the inhibitor concentration shift the corrosion potential to the positive values. This is due to the presence of the extract on the zinc surface and could be related to the delay of the corrosion reaction. The observation of figures 2 and 3 shows that the cathodic part is divided into two slices when the extract has been added to the medium. In general, there are two behaviours describing the cathodic reduction of oxygen: either this includes a direct transfer of four electrons (Eq. 1) or two consecutive steps with transfer of two electrons each. In this second case, the first step involves a reduction of hydrogen peroxide (Eq. 2) and then a further reduction (Eq. 3). These slices are well marked for the extract obtained by UAE, and are less for the extract obtained under reflux. This dissimilarity may be due to the difference of the extracts, which contain identical functional groups with a difference in the concentration of molecules. A peak appears at -1225 mV/SCE after *EEBGP* addition in the corrosive medium for all concentrations as shown in Figs. 2 and 3. This peak is due to the presence of a passive layer. According to Mouangua et al. [20] and Muster et al. [21], zinc is passivated by formation of $Zn_5(OH)_8Cl_2{\cdot}2H_2O$, due to the reduction of corrosion products [22].

$$O_2 + 2\,H_2O + 4\,\bar{e} \leftrightarrow 4\,OH^- \quad (1)$$

$$O_2 + 2\,H_2O + 2\,\bar{e} \leftrightarrow H_2O_2 + 2\,OH^- \quad (2)$$

$$H_2O_2 + 2\,\bar{e} \leftrightarrow 2\,OH^- \quad (3)$$

In the presence of the extract, a significant reduction was identified, this is probably due to a change in the reaction process, which would result in a decrease in current, but without change of the anode slope. The anodic branches have a very rapid increase of current with polarization explained by the potential desorption of the inhibitor near to the corrosion potential.

Lorenz and Mansfeld explain such comportment by an anodically impolarisable electrochemical system [23].

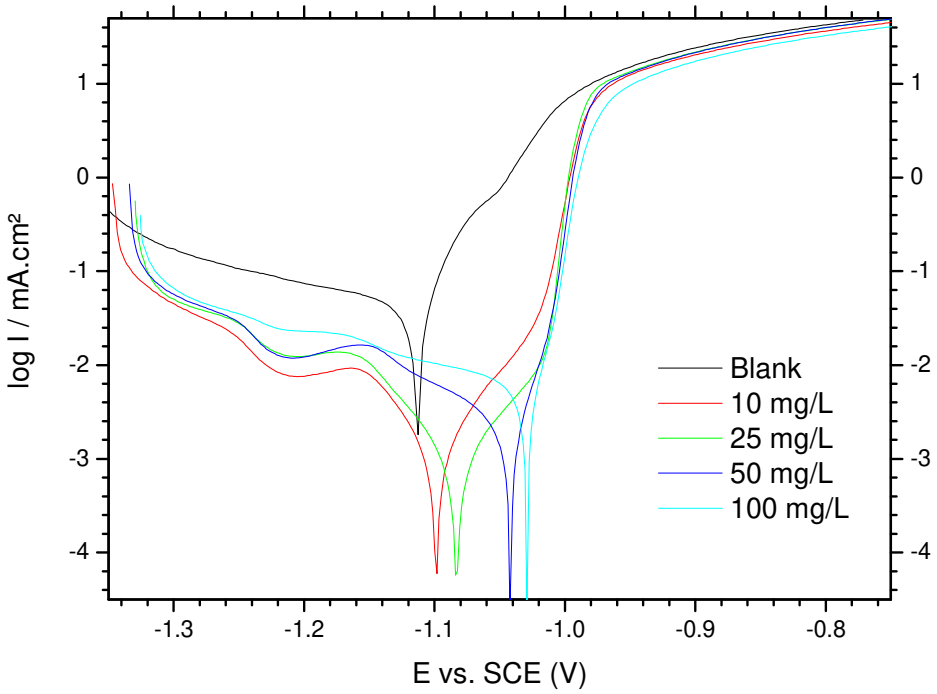

Fig. 2. Polarization curves for zinc in 3% NaCl in the presence of *EEBGP* obtained by UAE.

The inhibition efficiency values η_{RP} (%) calculation using Tafel curves (i_{corr}) is not possible, as the experimental polarization curves do not exhibit linear Tafel regions. Then η_{RP} (%) values were calculated from the polarization resistance (R_p) according to an earlier study [13]. The R_p values were obtained using linear *I–E* plots in the potential range ± 25 mV from the corrosion potential. It's found that R_p increases with the concentration. Also, we notice that when the C_{inh} increases, η_{Tafel}(%) also increases to reach a maximum value (97 %) at 100 ppm of *EEBGP*. We can conclude that the *Bagassa guianensis* extract is very effective inhibitor for the zinc corrosion in 3% NaCl even at lower concentration. The literature available according to our knowledge about the use of the plant extracts as green inhibitors for zinc corrosion in NaCl medium is very limited. Indeed, the evaluation of the *Mansoa alliacea* extract as green inhibitor against the zinc corrosion in the same experimental conditions showed that the maximum inhibition value of 92% was reached at 300 ppm [11]. El-Etre et al. were found that the aqueous

extract of lawsonia leaves acts as a good inhibitor for zinc corrosion in neutral medium (0.5 M NaCl) and attained 91% at 800 ppm [12].

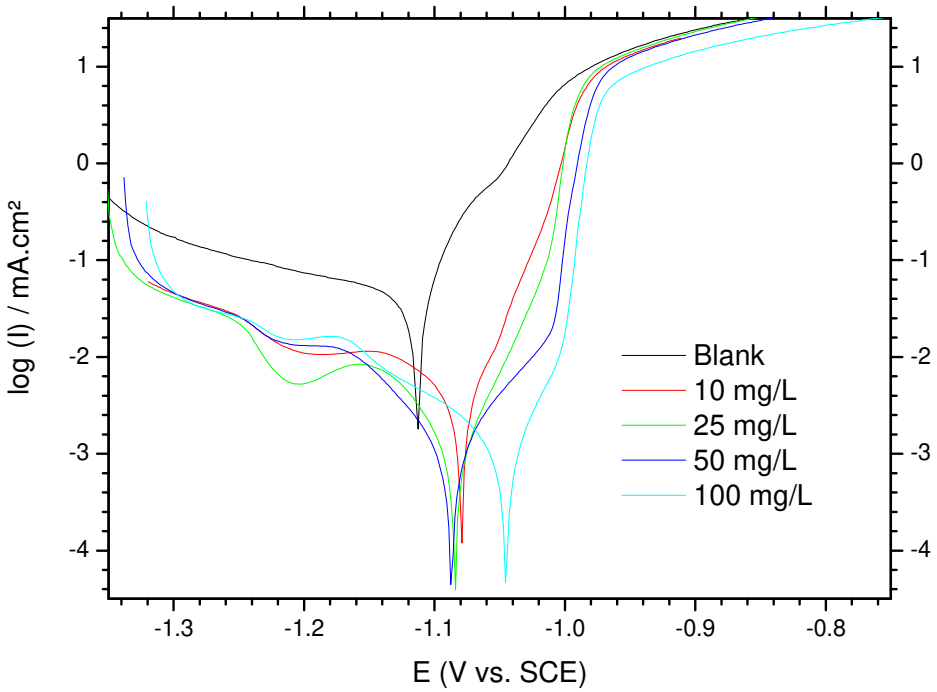

Fig. 3. Polarization curves for zinc in 3% NaCl in the presence of *EEBGP* obtained under reflux.

Table 1
Polarization parameters and the corresponding inhibition efficiency for the corrosion of zinc in 3% NaCl containing different concentrations of *EEBGP* at 25 °C.

Concentration (mg/L)	E_{corr} vs. SCE (V)	R_p (Ω cm^2)	η_{RP} (%)
3% NaCl	-1.113	518	—
UAE			
10	-1.093	2613	80
25	-1.075	11867	96
50	-1.078	22841	98
100	-1.057	17845	97
Reflux			
10	-1.065	2946	82
25	-1.082	8212	94
50	-1.104	10933	95
100	-1.073	13000	96

3.3. AC impedance results

The impedance plots of zinc in the presence of *EEBGP* are shown in Figs. 4 and 5.

Primary, the impedance plots of zinc in 3% NaCl has considerably affected by adding the extract and exhibited two depressed capacitive semicircles, throughout the frequency region, behaviour already reported by several authors [24,25]. The initial loop, in the high-frequency side, is associated to the charge transfer, while the second one is due to the diffusion process associated to the oxygen reduction. An adjustment of the obtained data was realized by the corresponding circuit given in Fig. 6. It should be noted that each equivalent circuit is adapted to the corresponding system with two or three phenomena. The circuit contains the solution resistance R_s, the charge transfer resistance (R_{ct}) and the constant phase element (CPE_{ct}) which is positioned in series to corrosion product resistance (R_{cp}) and the constant phase element (CPE_{cp}). At low concentration values (10-25 mg/L), the inhibitor concentration is insufficient to cover the entire surface, two regions could be considered. The first region where the inhibitor is absent, only charge transfer parameters R_{ct} and CPE_{ct} are considered. In addition, the second region where the inhibitor is present, a new time constant due to adsorption was used and characterized an adsorption resistance (R_a) and a phase constant element (CPE_a) in the equivalent circuit model; Fig. 6a. While at high concentration values the inhibitor quantity is sufficient to cover the entire surface, thus contributing to form a layer containing the corrosion products on the surface. In this case, the time constant characterized by the parameters R_{ct} and CPE_{ct} disappears. Fig. 7 shows a schematic representation of the phenomena at the interface as function of the extract concentration. Additionally, we note that a similar electrochemical behaviour was found for both extraction methods. It means that the extracts (obtained by both methods) do not depend on the extraction process used for corrosion protection of zinc.

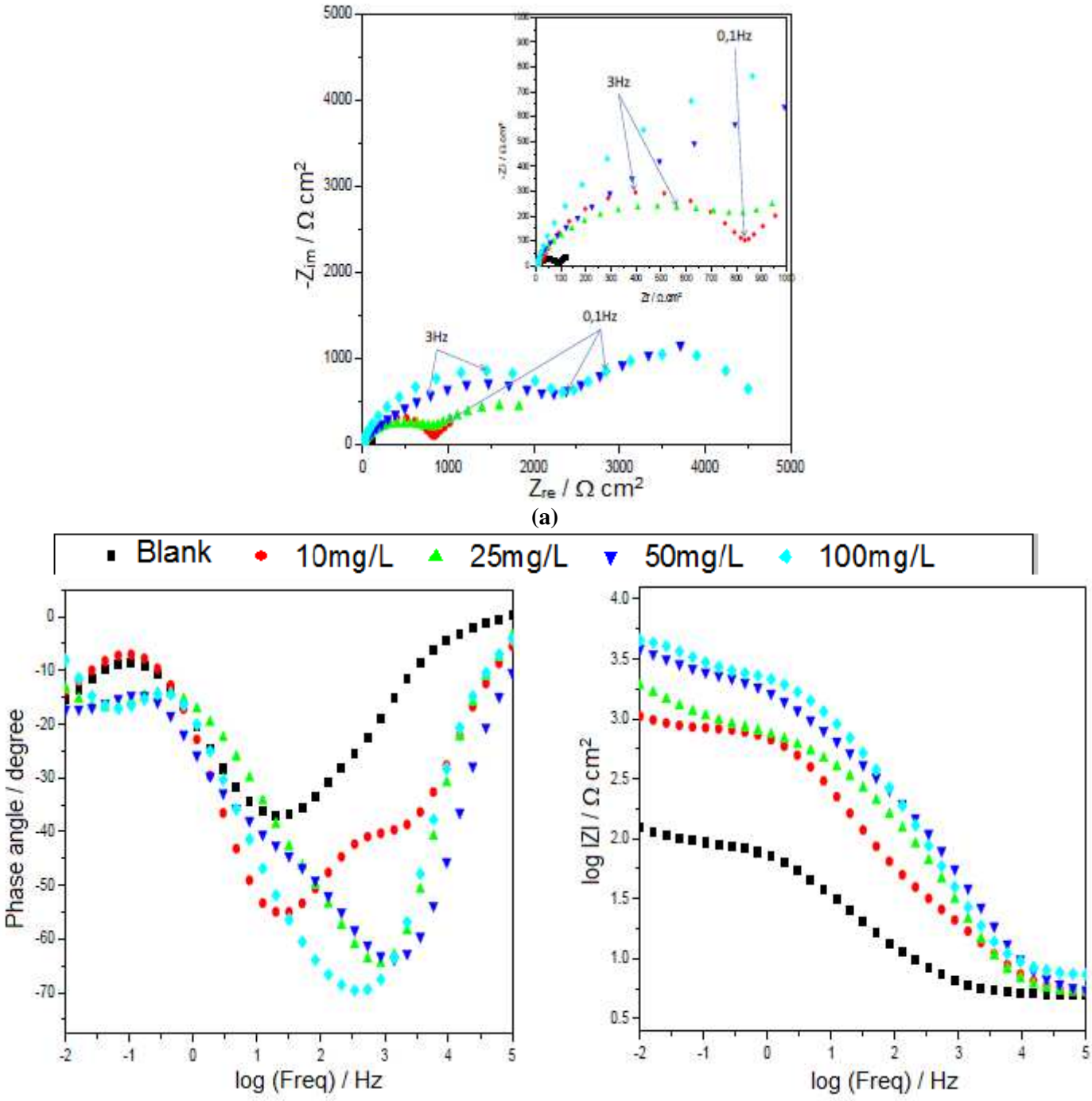

Fig. 4. Nyquist (a) and Bode (modulus (b) and phase (c)) diagrams for zinc in 3% NaCl in the presence of EEBGP obtained by UAE.

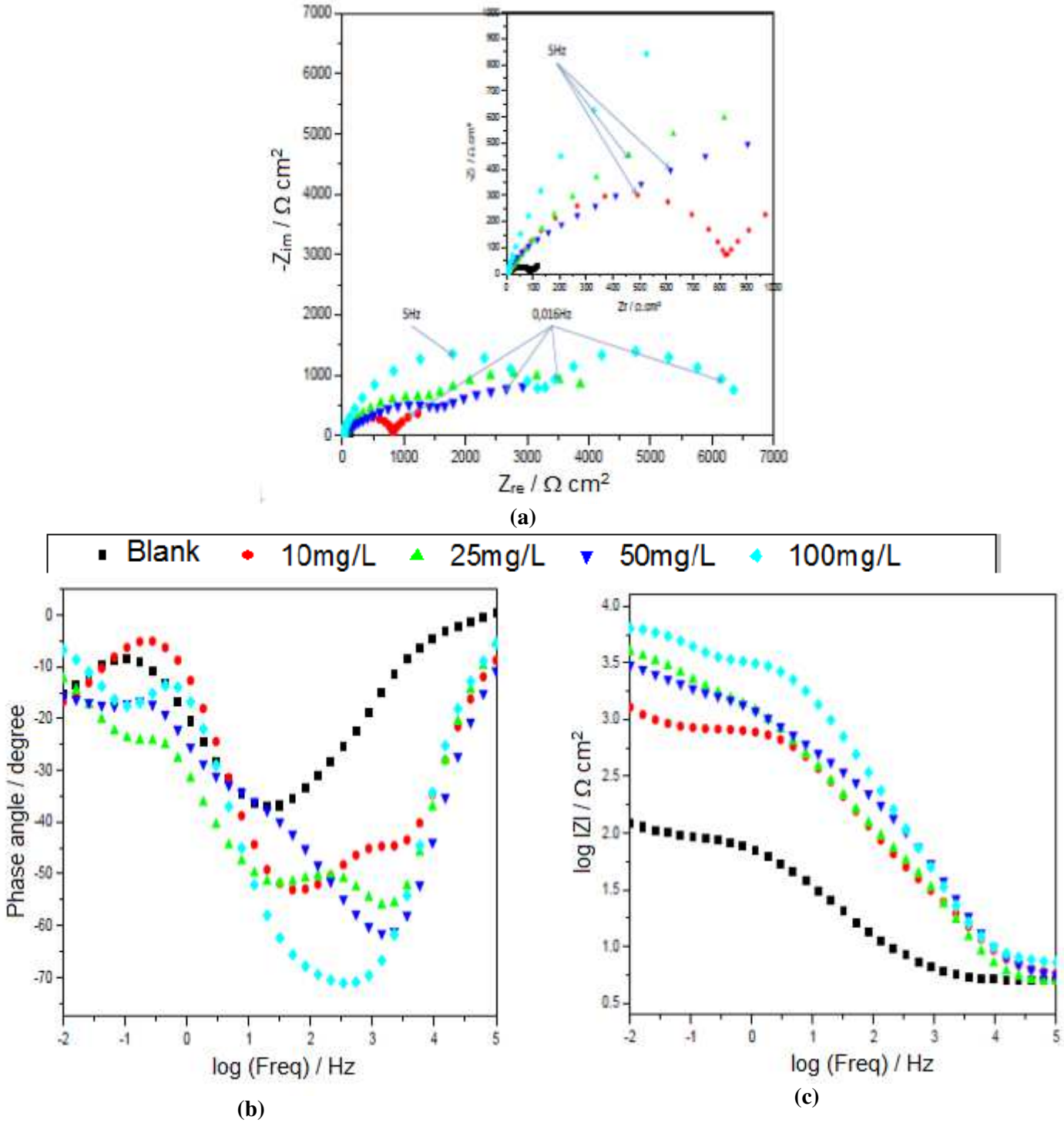

Fig. 5. Nyquist (a) and Bode (modulus (b) and phase (c)) diagrams for zinc in 3% NaCl in the presence of *EEBGP* obtained under reflux.

Ω

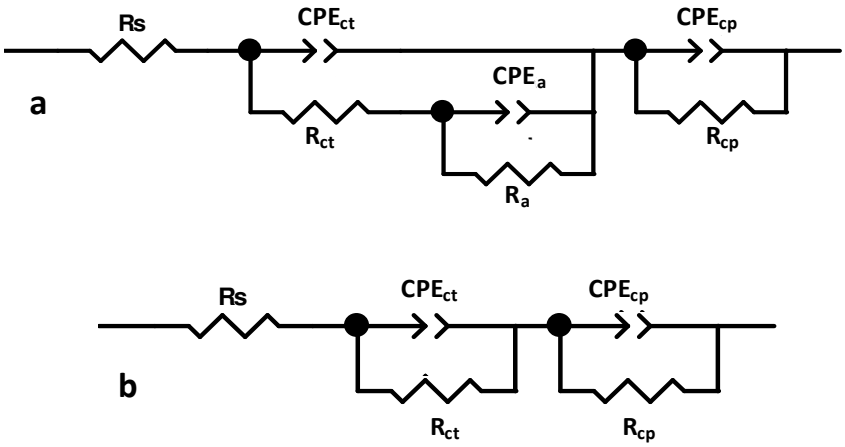

Fig. 6. Equivalent circuits employed for fitting the impedance diagrams data, (a) with 3 time constants and (b) with 2 time constants.

All the electrochemical parameters are exposed in the Tables 2 and 3. The R_s values are unaffected when adding extract. However, the total resistance (R_t) values ie. $R_{ct} + R_{cp} + R_a$ rises with the concentration which explains the increase in the η_Z % and also corroborates the proposed model in Fig. 7. The extracts have relatively close corrosion inhibition efficiency because of its same composition of organic compounds. The α values appear to be superior to those found for the corrosive medium, which indicates that the heterogeneity of the zinc surface is decreased by inhibitor adsorption. The Mansfeld formula was employed to evaluate the C_{dl} values [26-33]. The C_{dl} values are calculated only from graphical parameters α and Q according to Orazem et al. method [34-36]; Figs. 8 and 9. All the details and the method of calculation for graphical parameters are given in [18]. The α and Q graphical values and C_{dl} associated results are summarized in Table 4. Sometimes, the poor slope definition did not allow to measure α and Q, in particular at the most important inhibitor concentrations. Therefore, only two phenomena could be considered for the graphical method. The α values obtained from graphical method have the same evolution as those found by fit. The CPE Q and C_{dl} values decrease with rise in concentrations. Consequently, the first C_{dl} corresponds to charge transfer phenomenon and the last to the corrosion products layer.

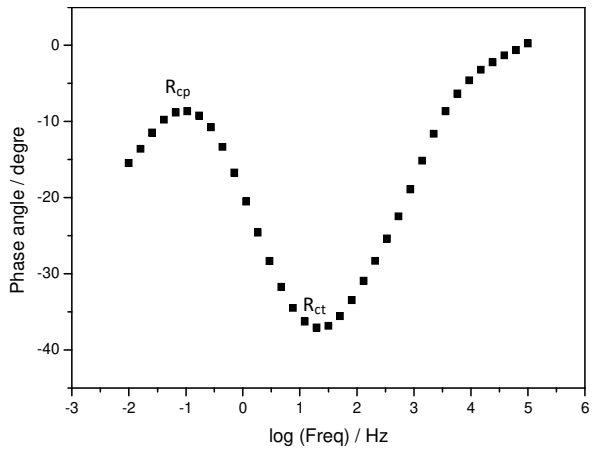

Corrosion products

(a)

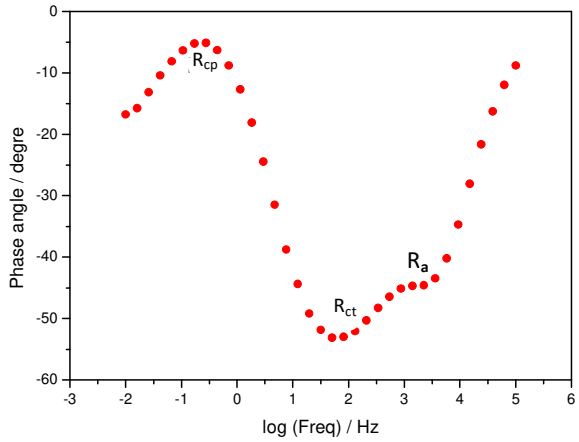

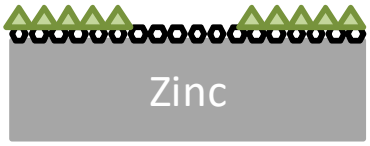

Inhibitors
Corrosion products

(b)

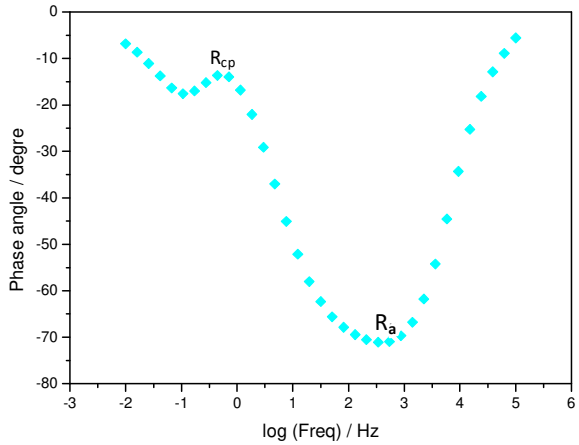

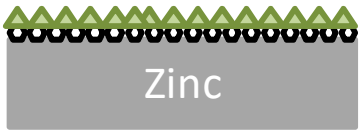

Inhibitors
Corrosion products

(c)

Fig. 7. Bode phase diagram for zinc in 3% NaCl and schematic describing the evolution of the covering of the zinc surface versus *EEBGP* concentration in 3% NaCl: (a) without inhibitor, (b) with addition of *EEBGP* and (c) with addition of optimum concentration of *EEBGP*.

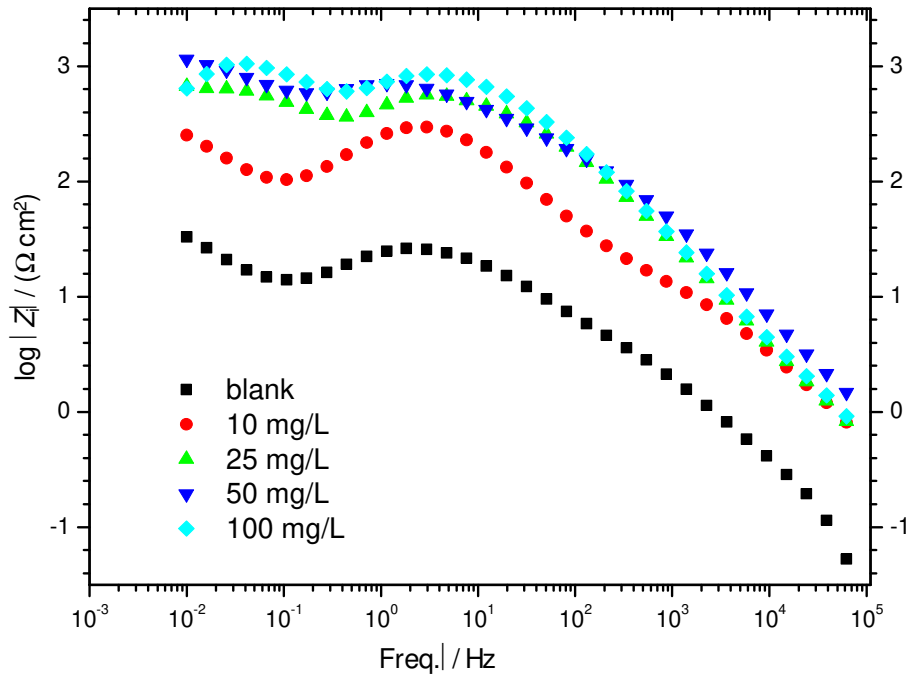

Fig. 8. Imaginary part of the impedance as a function of frequency using graphical method in the presence of different concentrations of *EEBGP* obtained by UAE.

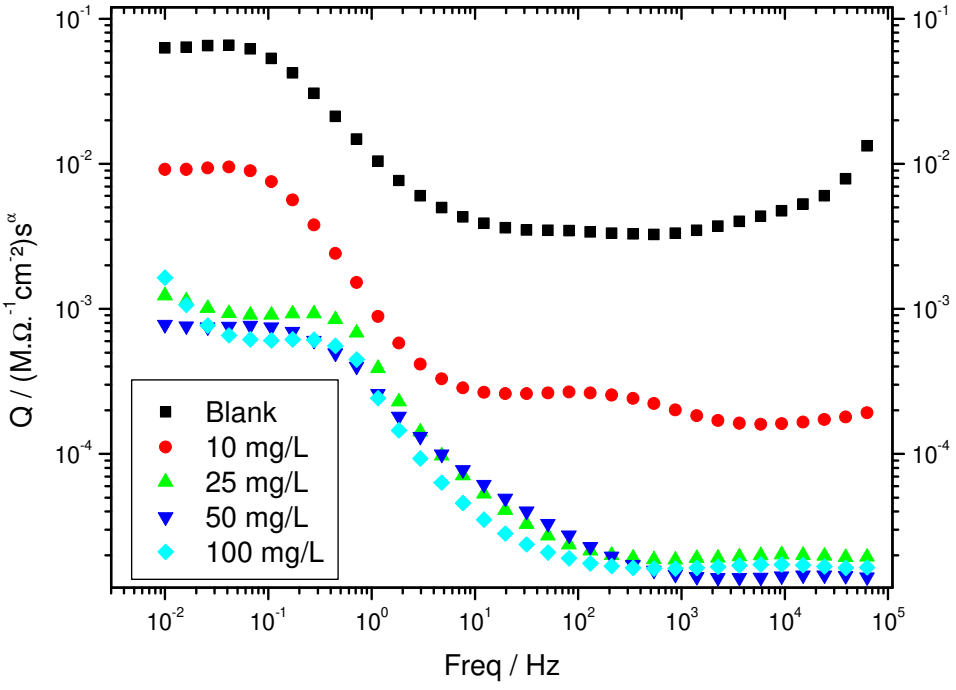

Fig. 9. Effective *CPE* coefficient calculated by the graphical method as a function of frequency in the presence of different concentrations of *EEBGP* obtained by UAE.

Table 2

Values of the fit obtained from the EIS data for zinc in 3% NaCl with and without different concentrations of *EEBGP* obtained by UAE.

Parameter	Blank	10 mg/L	25 mg/L	50 mg/L	100 mg/L
R_s (Ω cm^2)	5	5	5	5	7
Q_{ct} 10^{-4} (Ω^{-1} cm^{-2} s$^{\alpha}$)	20	0.8	0.1	0.1	—
α_{ct}	0.623	0.764	0.925	0.866	—
R_{ct} (Ω cm^2)	92	18	129	271	—
Q_{cp} 10^{-4} (Ω^{-1} cm^{-2} s$^{\alpha}$)	2020	348	44	30	20
α_{cp}	0.781	0.934	0.781	0.727	0.999
R_{cp} (Ω cm^2)	111	567	1223	3398	2034
Q_a 10^{-4} (Ω^{-1} cm^{-2} s$^{\alpha}$)	—	1.4	1.9	1	0.4
α_a	—	0.791	0.549	0.604	0.733
R_a (Ω cm^2)	—	830	795	2157	2610
θ	—	0.856	0.905	0.965	0.956
η_Z (%)	—	86	91	96	96

Table 3

Values of the fit obtained from the EIS data for zinc in 3% NaCl with and without different concentrations of *EEBGP* obtained under reflux.

Parameter	Blanc	10 mg/L	25 mg/L	50 mg/L	100 mg/L
R_s (Ω cm^2)	5	6	5	6	7
Q_{ct} 10^{-4} (Ω^{-1} cm^{-2} s$^{\alpha}$)	20	2	0.1	0.1	—
α_{ct}	0.623	0.609	0.915	0.854	—
R_{ct} (Ω cm^2)	92	254	59	214	—
Q_{cp} 10^{-4} (Ω^{-1} cm^{-2} s$^{\alpha}$)	2020	7.3	23	41	8.1
α_{cp}	0.781	0.290	1	0.793	0.906
R_{cp} (Ω cm^2)	111	559	1928	1953	3183
Q_a 10^{-4} (Ω^{-1} cm^{-2} s$^{\alpha}$)	—	0.7	1.3	1.8	0.2
α_a	—	1	0.656	0.549	0.826
R_a (Ω cm^2)	—	296	1996	1773	3355
θ	—	0.817	0.949	0.948	0.969
η_Z (%)	—	82	95	95	97

Table 4

The graphical method parameters in the presence of of *EEBGP* obtained by UAE.

Parameters	Blank	10 mg/L	25 mg/L	50 mg/L	100 mg/L
Q_{ct} 10^{-6} (Ω^{-1} cm^{-2} s^{α})	35	2	0.2	0.2	0.3
α_{ct}	0.542	0.632	0.862	0.802	0.829
C_{dl} (μF cm^{-2})	115	3.6	4.6	2.1	5.2
Q_a 10^{-4} (Ω^{-1} cm^{-2} s^{α})	644	172	46	62	53
α_a	0.432	0.751	0.908	0.793	0.841
C_a (mF cm^{-2})	1.5	7.6	3.1	2.5	2.8

3.4. Adsorption behaviour and surface analysis

Adsorption isotherms are also an important complement that can help to understand the mode of action of inhibitory molecules on the metal surface. The following isotherms expressions were verified for the inhibitor extract:

$$\frac{C_{inh}}{\theta} = \frac{1}{K_{ads}} + C_{inh} \quad \text{(Langmuir isotherm)} \quad (4)$$

$$\exp(-2a\theta) = K_{ads}C_{inh} \quad \text{(Temkin isotherm)} \quad (5)$$

$$\left(\frac{\theta}{1-\theta}\right)\exp(2a\theta) = K_{ads}C_{inh} \quad \text{(Frumkin isotherm)} \quad (6)$$

The values of θ can be easily determined by from AC impedance results by $\eta_Z(\%)$ / 100. Based on the values of correlation coefficient (R^2), it is evident that the Langmuir was the best fit model for the adsorption of *EEBGP* molecules on zinc surface (Fig. 10) for which the R^2 values were found to be equal to 1 and 0.996 using ultrasound-assisted extraction and under reflux method, respectively. However, the R^2 values are equal to 0.87 and 0.77 in the case of Temkin and to 0.21 and 0.01 in the case of Frumkin isotherm, using ultrasound-assisted extraction and under reflux method, respectively. The Langmuir isotherm exhibits single-layer adsorption characteristic, assuming that no interaction between the adsorbed molecules on the zinc surface.

However, this behaviour subsists speculative in the case of plant extracts, simply because to the intermolecular effects (electronic and steric) of different active constituents present in the investigated extract.

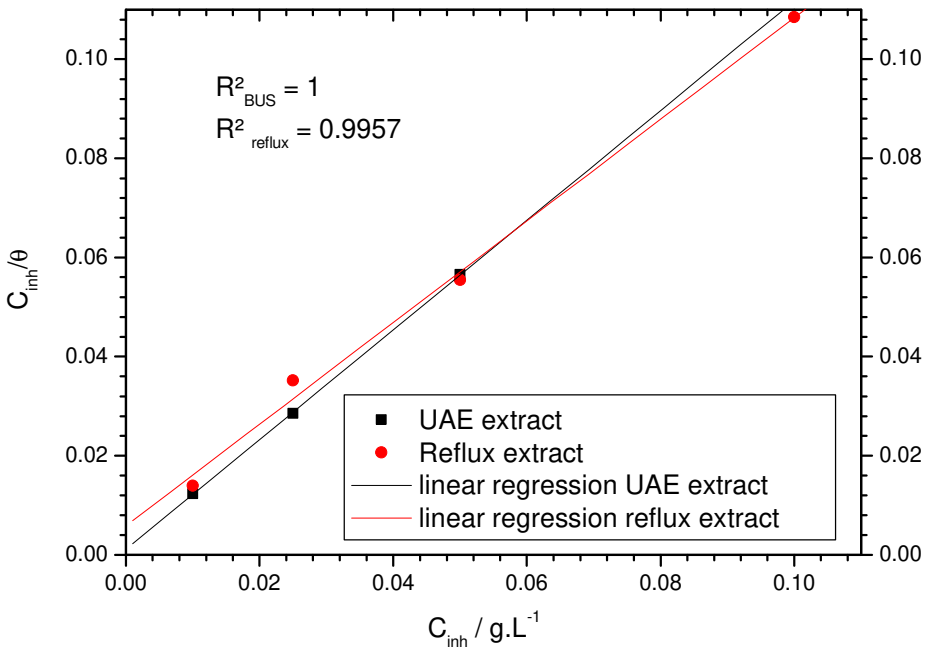

Fig. 10. Langmuir isotherm for zinc in 3% NaCl in the presence of *EEBGP* at 25°C.

X-ray photoelectron spectroscopy (XPS) analysis was employed to further study the adsorption mechanism of *EEBGP* on the zinc surface and to provide insight into the chemical nature of the adsorbed film on the substrate surface. The XPS analyses were performed on the *EEBGP* and the zinc substrate subsequent to 4h of immersion in 3% NaCl medium with 100 mg/L of *EEBGP*. The obtained XPS spectra are given in Figs. 11 and 12 and the deconvoluted data are summarised in Table 5.

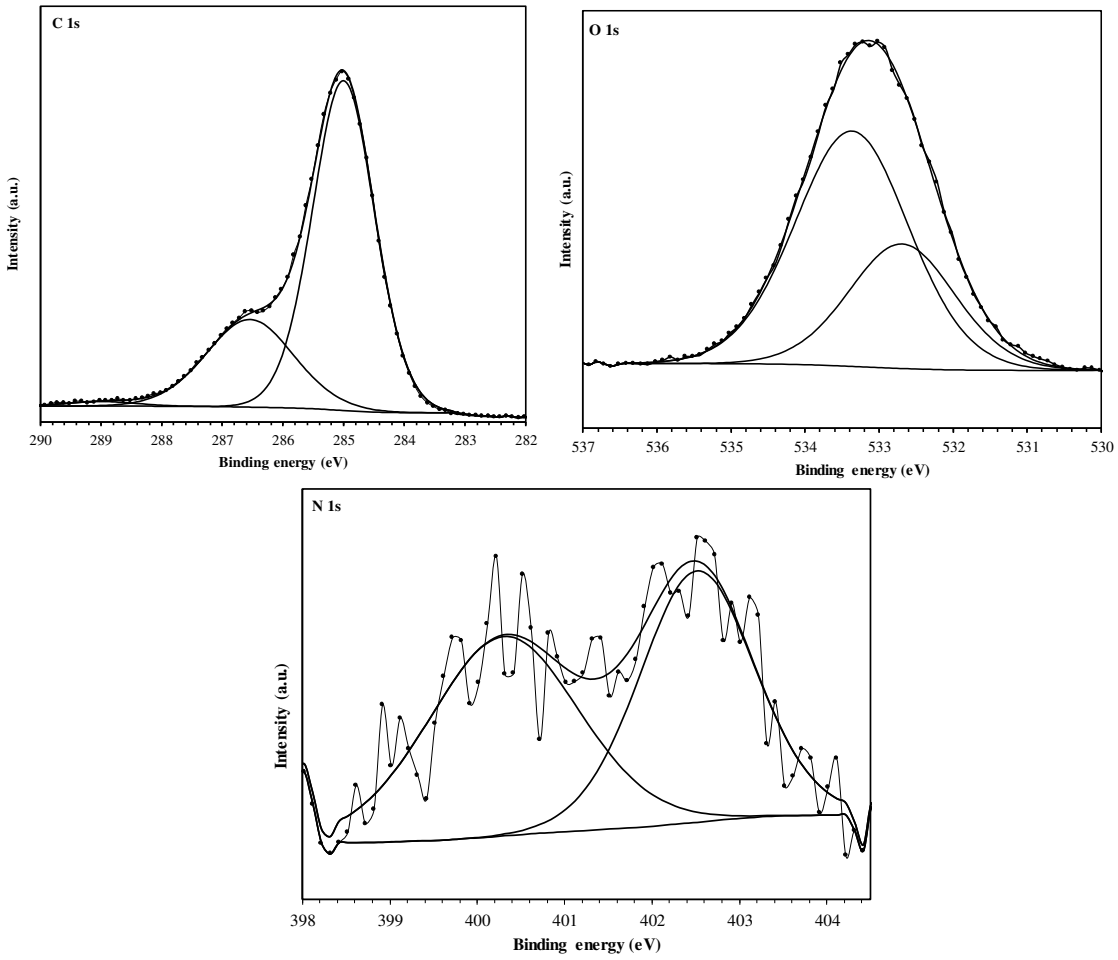

Fig. 11. C 1s, O 1s and N 1s XPS deconvoluted profiles for *Bagassa guianensis* plant extract (*EEBGP*).

The deconvolution of the C 1s spectrum for *EEBGP* may be fitted into three components at 285, 286.5 and 289 eV (Fig. 11, Table 5). The first pic can be attributed to contaminant hydrocarbons and to the C–C, C=C and C-H bonds [37], the second may mainly assigned to the C–O and C=O bonds, and can be also associated with the presence of C–N and C=N bonds [38], and the latest can be ascribed to C=O and COO bonds. The O 1s spectrum for *EEBGP* could be fitted into two main constituents at 532.7 and 533.4 eV Ev (Fig. 11, Table 5), may be attributed to C–O and C=O bonds [39,40]. It should be noted that the low signal intensities from the N 1s XPS spectrum for *EEBGP* (Fig. 11) cannot be used to detect the chemical composition. This is due to the low presence of nitrogen atom in the extract. However, the elemental composition from XPS confirm the low percent of nitrogen (0.75%) due to the low content of alkaloid

molecules in the *Bagassa guianensis* plant extract. The N 1s XPS spectrum for *EEBGP* is fitted into two components (Fig. 11, Table 5) located at 400.3 and 402.5 eV. Indeed, the first pic is principally assigned to the C–N and the unprotonated N atom (=N– structure) and the second one and could be related to protonated nitrogen atoms ($=N^{+}H-$) [41,42].

After immersion in 3% NaCl containing 100 mg/L of *EEBGP*, high-resolution C 1s spectrum of zinc surface can be deconvoluted into three components (Fig. 12, Table 5). The first one at 285.0 eV is attributed to contaminant hydrocarbons and to the C–C, C=C and C–H bonds, the second at 286.6 eV may be mainly assigned to the C atom in C–O and C=O bonds. The latest at a higher binding energy (288.9 eV) can be ascribed to C atom of C=O and of COO. The N 1s spectrum of *EEBGP*-treated zinc surface reveals also a low signal intensity in the same binding energies range. However, the low nitrogen content (0.8 %) remains unchanged on the zinc surface. This result can be explained by the low content of alkaloid molecules in the *Bagassa guianensis* plant extract (*EEBGP*).

For the O 1s signal, the corresponding spectrum could be fitted into two components located at 532.2 and 533.4 eV (Fig. 12, Table 5). The first component can be associated to the presence of zinc hydroxide species such as $Zn(OH)_2$ and/or $Zn_5(OH)_8Cl_2{\cdot}2H_2O$ [43,44], while the second one can be attributed to oxygen of adsorbed water [45]. These two components may be also attributed to oxygen in C=O and in C–O bonds in *EEBGP* molecules [46], indicating that the *EEBGP* molecules are adsorbed on the zinc surface. High-resolution Zn 2p spectrum (Fig. 13) depicts a double peak profile located at 1022.7 eV (Zn $2p_{3/2}$) and 1045.7 eV (Zn 2p1/2). The deconvolution of the Zn $2p_{3/2}$ XPS spectrum consists in two components (Fig. 12, Table 5), the small one at 1021.1 eV is attributed to metallic zinc [47], while the second component at 1022.7 eV can be associated to zinc hydroxide species [48]; this finding is in agreement with the presence of the zinc hydroxide as detected in the O 1s spectrum. The obtained XPS results give evidence of chemical interactions between the *EEBGP* inhibitor and zinc surface in 3% NaCl

medium. Indeed, the presence of oxygen species (C–O, C=O) on the zinc surface, confirms that the investigated plant extract can be occurred directly by a chemisorption process on the zinc surface.

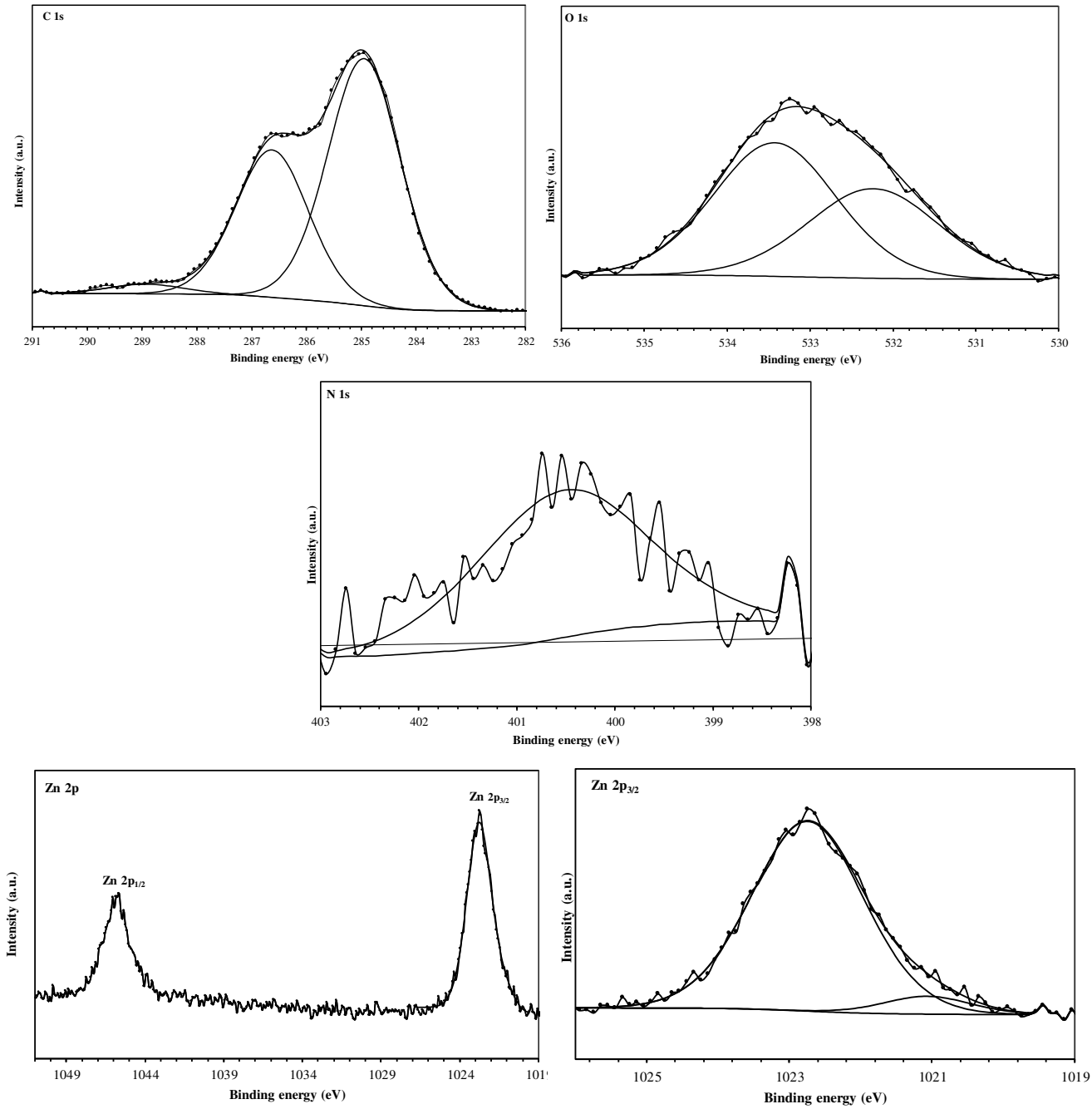

Fig. 12. C 1s, O 1s, N 1s, and Zn 2p XPS deconvoluted profiles for zinc surface treated with *EEBGP* in 3% NaCl at 25 °C.

Table 5
Binding energies (eV), relative intensity and their assignment for the major core lines observed *EEBGP* and zinc substrate treated with *EEBGP* in 3% NaCl at 25°C.

Substrate	C 1s		N 1s		O 1s		Zn $2p_{3/2}$	
	BE (eV)	Assignment	BE (eV)	Assignment	BE (eV)	Assignment	BE (eV)	Assignment
EEBGP	285.0 (72 %)	C–C/C=C/C–H	400.3 (51 %)	=N– structure/ C–N	532.7 (33 %)	C–O/C=O/OH	—	—
	286.5 (27 %)	C–O/C=O/ C=N/C–N	402.5 (49 %)	—	533.4 (67 %)	C–O/C=O	—	—
	289.0 (1 %)	C=O/COO	—	—	—	—	—	—
EEBGP treated zinc substrate	285.0 (61 %)	C–C/C=C/C–H	400.5 (100 %)	=N– structure, C–N	532.2 (42 %)	$Zn(OH)_2$/C–O/C=O	1021.1 (7 %)	Zn^0
	286.6 (37 %)	C–O/C=O/ C=N/C–N	—	—	533.4 (58 %)	C–O/C=O/H_2O_{ads}	1022.7 (93 %)	zinc hydroxide species
	288.9 (2 %)	C=O/COO	—	—	—	—	—	—

3.5. Phytochemical studies

An additional study was carried out combining evaluation, quantification and qualification of the extract. First, the various chemical families present in the extract have been identified through phytochemical tests. Then, these chemical families were separated and quantified. Secondly, the inhibition activity of the isolated families was evaluated. The objective of this study is to identify the main constituent of the extract responsible for inhibition.

Phytochemical tests realized on the crude extract detect the appearance of diverse chemical families with dissimilar proportion (Table 6). Each chemical family was isolated individually, collected and weighted (UHPLC). HPLC spectroscopy spectra indicate that each fraction (chemical families) enclosed a combination of several organic elements (only one illustrative sample is shown here in Fig. 13). It should be noted that, it was very difficult to get the composition of each family.

Table 6

The ratio of diverse families of *EEBGP* and their EIS data.

Compound	Ratio	R_t (R_{ct}+R_{cp}) (Ω cm^2)	η_Z (%)
Blank	—	203	—
Anthocyans	16%	539	62
Coumarins	7%	384	47
Flavonoids	23%	3585	94
Quinons	2%	915	78
Saponins	36%	1700	88
Tanins	9%	666	69
Triterpens	7%	552	63
Total extract	100%	2357	91

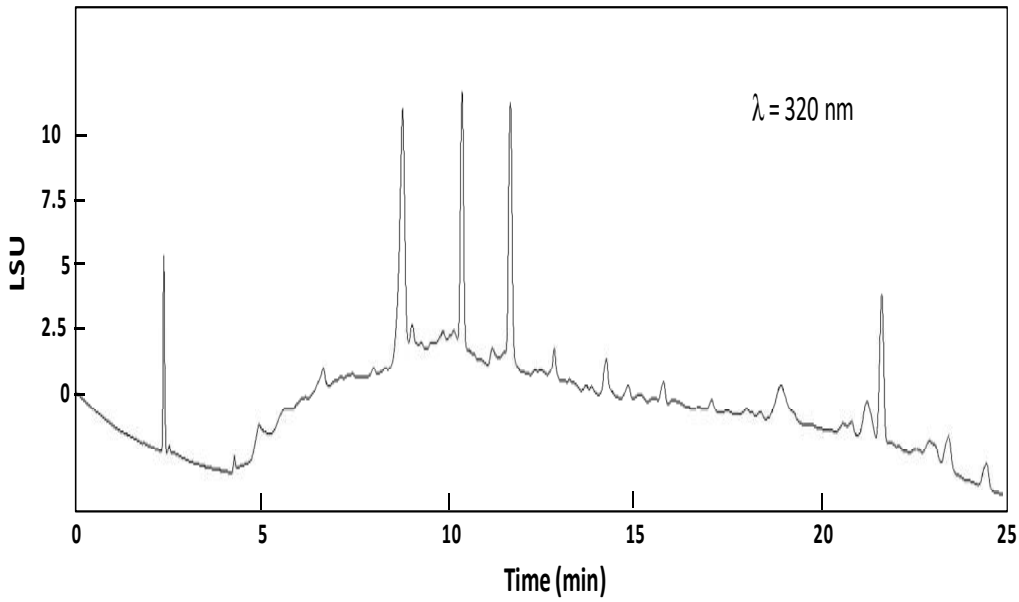

Fig. 13. HPLC chromatogram of total anthocyans extract from the crude extract.

The inhibitive effect of each family was evaluated and comparted to the total extract (Fig. 14). The obtained results illustrate that all the diverse chemical families inhibit the corrosion. To note that flavonoids family was found more effective than total extract. One can conclude that the family responsible for the inhibitory activity is the flavonoids.

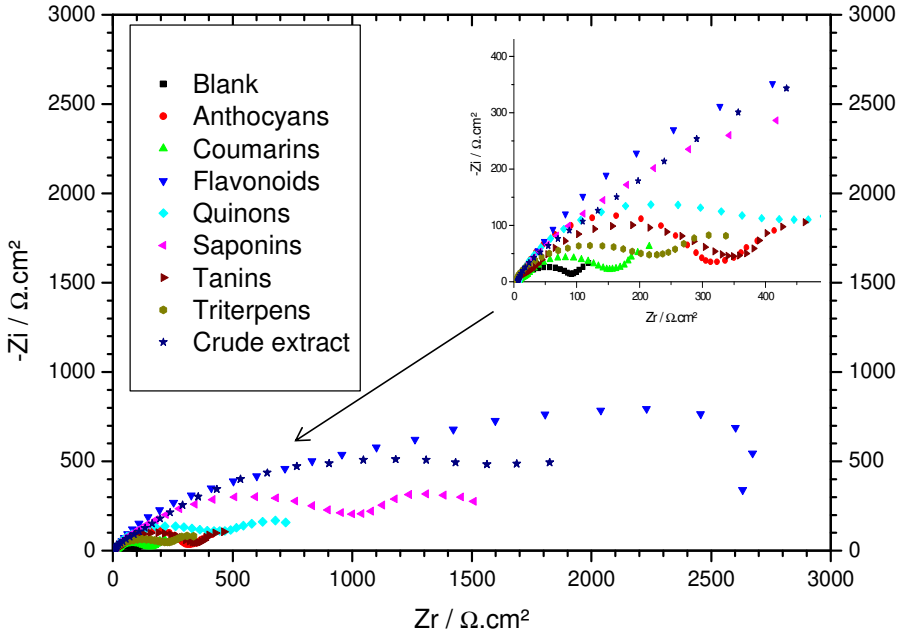

Fig. 14. Nyquist plots for zinc in 3% NaCl medium containing different families and the crude extract.

As the flavonoids are the main constituent of the crude extract, a XPS study of this

family was realised to compare the adsorption of the crude extract (*EEBGP*) to that of flavonoids. Figs. 15 and 16 show the obtained XPS spectra (C 1s, O 1s, and Zn 2p core levels) for the isolated flavonoids and for the zinc surface after immersion in 3% NaCl solution with 20 mg/L of isolated flavonoids. Isolated flavonoids are nitrogen-free and the chemical structures of the major constituents of this family are given in the Fig. 17 as described previously by Royer et al. [49].

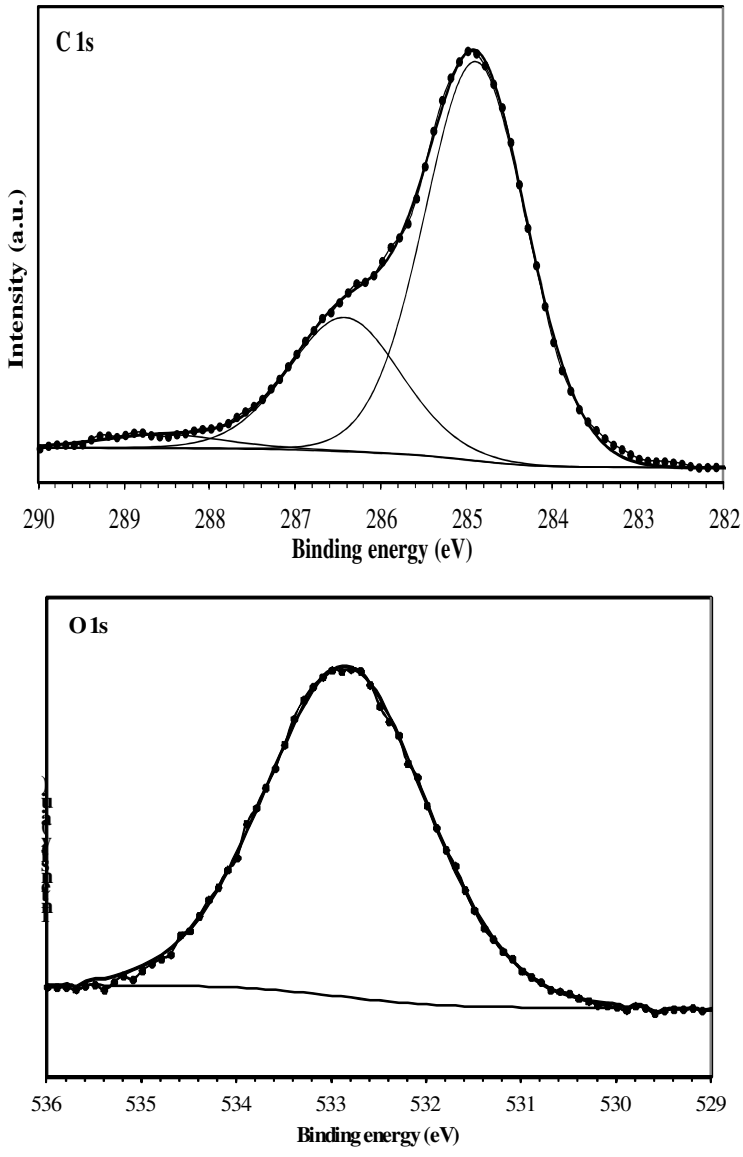

Fig. 15. C 1s and O 1s XPS deconvoluted profiles for flavonoids family.

The C 1s spectrum for the isolated flavonoids can be decomposed into three

components (Fig. 15, Table 7). The largest component can be attributed to contaminant hydrocarbons and to the C–C, C=C and C–H aromatic bonds with characteristic binding energy of 285.0 eV; the second component at 286.4 eV may be assigned to the C atom bonded in C–O and to C=O; the latest and the smaller at 288.8 eV may be ascribed to the C=O. In the O 1s spectrum, the single peak at 532.8 eV is attributed to C–O and to C=O in the flavonoid molecules (Fig. 17). After immersion in 3% NaCl medium containing 20 mg/L of isolated flavonoids, the deconvolution of Zn $2p_{3/2}$ XPS spectrum presents one component at 1022.6 eV (Fig. 16, Table 7), which can mainly be associated to the zinc hydroxide species cited previously. This result is confirmed by the O 1s finding. Indeed, the deconvolution of O 1s spectrum gives two main components at 531.9 and 533.2 (Fig. 16, Table 7). The first one corresponds to the OH^- ions in zinc hydroxide as detected in the Zn $2p_{3/2}$ [50], while the second component may be attributed to adsorbed water. The two O 1s components may be also related to O atom in C–O and C=O in the flavonoid molecules. Indeed, the C 1s spectrum shows the presence of the flavonoid molecules on the zinc surface (Fig. 16, Table 7). The XPS findings show characteristic bands of the flavonoid molecules on the Zn surface, indicating that the inhibition mechanism of flavonoids against the zinc corrosion is mainly based on the chemisorption.

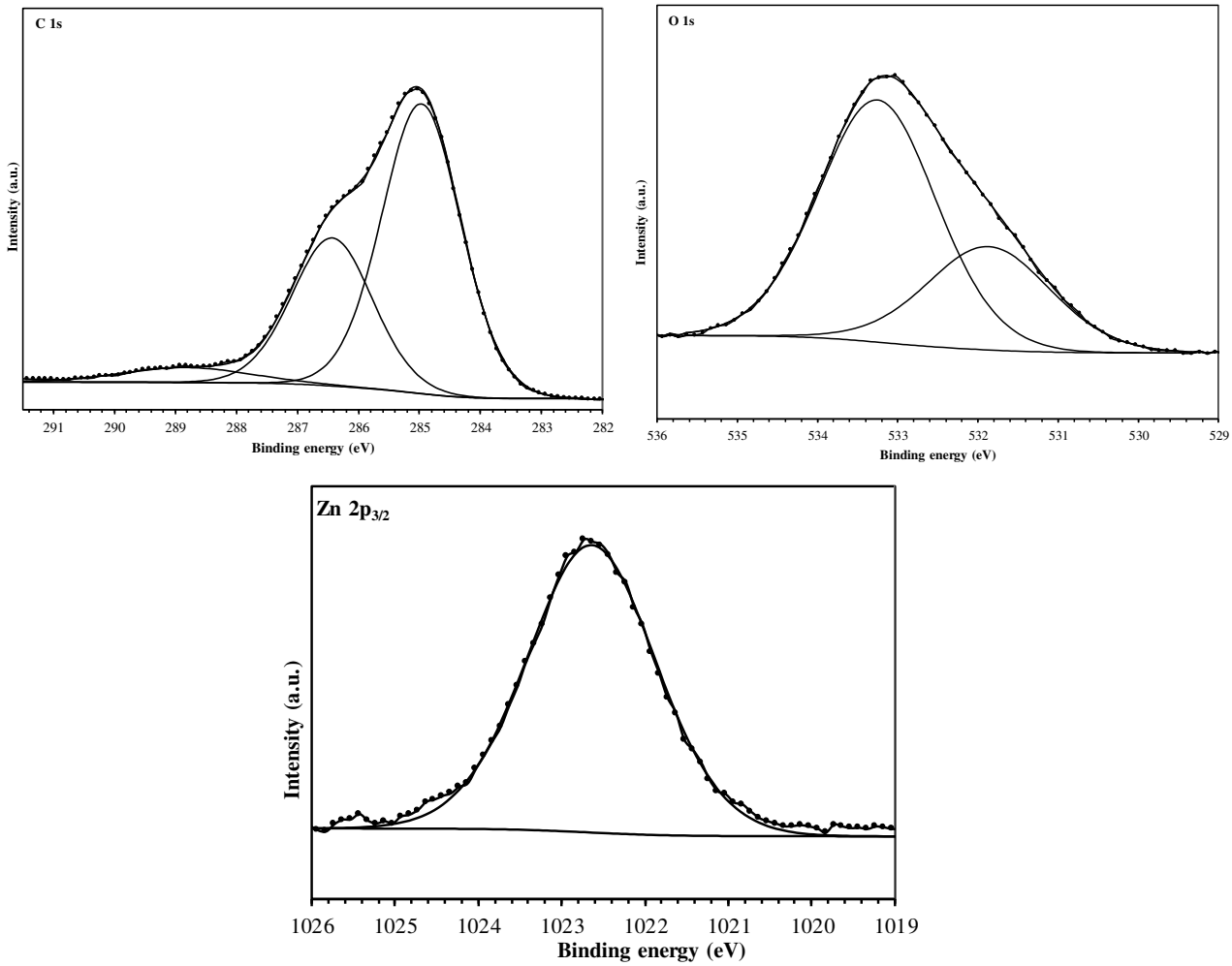

Fig. 16. C 1s, O 1s, and Zn 2p XPS deconvoluted profiles for Zinc surface treated with flavonoids in 3% NaCl at 25 °C.

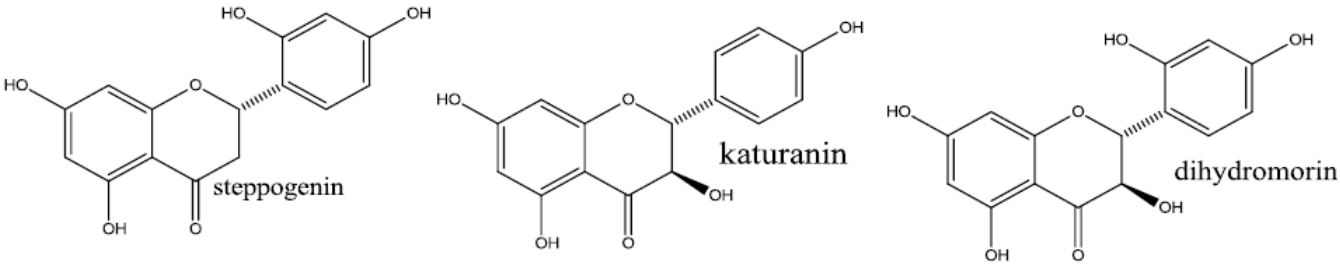

Fig. 17. Chemical structures of the major constituents of flavonoids family.

Table 7
The C 1s, O 1s and Zn $2p_{3/2}$ XPS profiles obtained for flavonoids and the submerged zinc in 3% NaCl with flavonoids at 25°C.

Substrate	C 1s		O 1s		Zn $2p_{3/2}$	
	BE (eV)	Assignment	BE (eV)	Assignment	BE (eV)	Assignment
Flavonoids	285.0 (71 %)	C–C/C=C/C–H	532.8 (100 %)	C–O/OH/ C=O	—	—
	286.4 (26 %)	C–O/C=O/	—	—	—	—
	288.6 (3 %)	C=O/COO	—	—	—	—
Flavonids treated zinc substrate	285.0 (62 %)	C–C/C=C/C–H	531.9 (31 %)	$Zn(OH)_2$/C–O	1022.6 (100 %)	zinc hydroxide species
	286.4 (33 %)	C–O/C=O/	533.2 (69 %)	C–O/C=O/ H_2O_{ads}	—	—
	288.8 (5 %)	C=O/COO	—	—	—	—

It should be noted that a physical mechanism can be also favourable especially the presence of the hydroxyl group which can cause a displacement of hydrogen atom with a pair of electrons in alkaline medium (at pH > 6). This rearrangement contributes to tautomerization and resonance structures (Fig. 18). Thus, flavonoids can adsorb directly via electrostatic interactions.

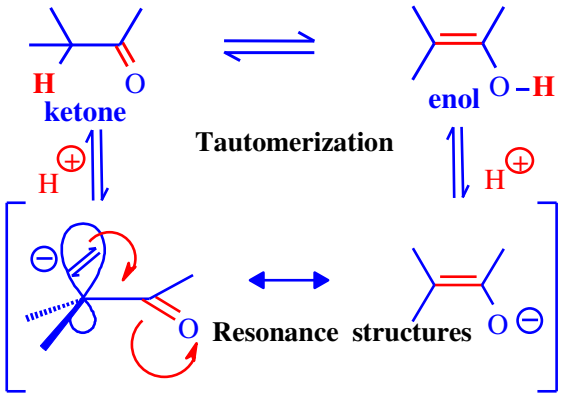

Fig. 18. Tautomerization and resonance structures of flavonoids.

4. Conclusions

The plant extract of *Bagassa guianensis* was found to be a good, original and eco-friendly corrosion inhibitor of zinc in sodium chloride solution. Two methods of extraction using as cheap and green solvent, were employed for such purpose. It was shown that the plant extract is an anodic-cathodic inhibitor according to the polarization findings. The impedance study showed the presence of two capacitive loops which involved a charge-transfer and a passive layer. The *CPE* parameters values obtained from graphical method have the same evolution as those found by fit. Langmuir isotherm describes well the adsorption behaviour of the studied extract. Phytochemical experiments detect the presence of diverse chemical families with dissimilar proportion. It was also demonstrated through the electrochemical experiments that the all diverse chemical families had the same behaviour as the total extract. However, it is mainly the flavonoid family that dominates the inhibitory activity. The XPS results indicated the founding of protective film inclosing the *Bagassa guianensis* extract and the flavonoids onto the zinc surface.

References

[1] K.H.J. Buschow, R. Cahn, M. Flemings, B. Ilschner, E. Kramer, S. Mahajan, Encyclopedia of Materials Science and Technology, vol. 7, Pergamon Press, New York, 2001.
[2] F.C. Porter, Zinc Handbook: Properties, Processing, and Use in Design, Marcel Dekker, New York, 1991.
[3] M. Abdalah, Corros. Sci. 45 (2003) 2705–2716.
[4] G. Trabanelli, Corros. 47 (1991) 410–419.
[5] D.S. Zhang, L.D. Li, L.X. Cao, N.F. Yang, C.B. Huang, Corros. sci. 43 (2001) 1627–1636.
[6] S. Manov, A.M. Lamazouere, L. Aries, Corros. Sci. 42 (2000) 1235–1248.
[7] K. Aramaki, Corros. Sci. 43 (2001) 1985–2000.
[8] Y.K. Agrawal, J.D. Talati J D, M.D. Shah, M.N. Desai, N.K. Shah, Corros. Sci. 46 (2004) 633–651.
[9] J. Dobryszycki,S. Biallozor, Corros. Sci. 43 (2001) 1309–1319.
[10] Y. Qiang, S. Zhang, L. Guo, S. Xu, L. Feng, I.B. Obot, S. Chen, J. Clean. Prod. 152 (2017) 17–25.
[11] F. Suedile, F. Robert, C. Roos, M. Lebrini, Electrochim. Acta 133 (2014) 631–638.
[12] A.Y. El-Etre, M. Abdallah, Z.E. El-Tantawy, Corros. Sci. 47 (2005) 385–395
[13] H. Nady, Egypt. J. Petrol. 26 (2017) 905–913.
[14] M. Royer, G. Herbette, V. Eparvier, J. Beauchêne, B. Thibaut, D. Stien, 71 (2010) 1708–1713.
[15] M. Royer, A.M.S. Rodrigues, G. Herbette, J. Beauchêne, M. Chevalier, B. Hérault, B. Thibaut, D. Stien, Int. Biodeter. Biodegr. 70 (2012) 55–59.
[16] P. Grenand, C. Moretti, H. Jacquemin, M. Prevost, Pharmacopées traditionnelles en Guyane: Créoles, Wayapi, Palikur, IRD, Paris, 2004.
[17] J.-A. Botosoa, Purification et Caractérisation chimique et biologique des principes actifs des extraits de feuilles de *Pechia madagascariensis* (Apocynaceae), in: Biochimie Fondamentale et Appliquée, Université d'Antananarivo, 2010.
[18] M. Chevalier, F. Robert, N. Amusant, M. Traisnel, C. Roos, M. Lebrini, Electrochim. Acta 131 (2014) 96–105.
[19] D.A. Shirley, Phys. Rev. B 5 (1972) 4709–4714.
[20] M. Mouanga, P. Berçot, J.Y. Rauch, Corros. Sci. 52 (2010) 3984–3992.
[21] T.H. Muster, I.S. Cole, Corros. Sci. 46 (2004) 2319–2335.
[22] H.J. Flitt, D.P. Schweinsberg, Corros. Sci. 52 (2010) 1905–1914.
[23] W.J. Lorenz, F. Mansfeld, Corros. Sci. 21 (1981) 647–672.
[24] M. Mouanga, P. Berçot, Corros. Sci. 52 (2010) 3993–4000.
[25] M. Mouanga, P. Berçot, J.Y. Rauch, Corros. Sci. 52 (2010) 3984–3992.
[26] S.P. Harrington, T.M. Devine, J. Electrochem. Soc. 155 (2008) C381–C386.
[27] S.P. Harrington, T.M. Devine, J. Electrochem. Soc. 156 (2009) C154–C159.
[28] V.D. Jovic, B.M. Jovic, Corros. Sci. 50 (2008) 3063–3069.
[29] T. Van Schaftinghen, C. Le Pen, H. Terryn, F. Hörzenberger, Electrochim. Acta 49 (2004) 2997–3004.
[30] M.L. Zheludkevich, R. Serra, M.F. Montemor, K.A. Yasakau, I.M.M. Salvado, M.G.S. Ferreira, Electrochim. Acta 51 (2005) 208–217.
[31] T. Van Schaftinghen, C. Deslouis, A. Hubin, H. Terryn, Electrochim. Acta 51 (2006) 1695–1703.
[32] K.A. Yasakau, M.L. Zheludkevich, O.V. Karavai, M.G.S. Ferreira, Prog. Org. Coat. 63 (2008) 352–361.
[33] M.L. Zheludkevich, K.A. Yasakau, S.K. Poznyak, M.G.S. Ferreira, Corros. Sci. 47 (2005) 3368–3383.
[34] M.E. Orazem, N. Pébère, B. Tribollet, J. Electrochem. Soc. 153 (2006) B129–B136.
[35] M. Musiani, M. Orazem, B. Tribollet, V. Vivier, Electrochim. Acta 56 (2011) 8014–8022.
[36] B. Hirschorn, M.E. Orazem, B. Tribollet, V. Vivier, I. Frateur, M. Musiani, Electrochim. Acta 55 (2010) 6218–6227.
[37] D. Briggs, M.P. Seah, Practical Surface Analysis by Auger and X-ray Photoelectron Spectroscopy, John Wiley & Sons Ltd., Sussex, 1983 (Section 9.4 and Appendix 2).

[38] M. Outirite, M. Lagrenée, M. Lebrini, M. Traisnel, C. Jama, H. Vezin, F. Bentiss, Electrochim. Acta 55 (2010) 1670–1681.
[39] A.G. Kannan, N.R. Choudhury, N.K. Dutta, Polymer 48 (2007) 7078–7086.
[40] R.D. Boyd, J. Verran, K.E. Hall, C. Underhill, S. Hibber5t, R. West, Appl. Surf. Sci. 172 (2001) 135–143.
[41] O. Olivares-Xometl, N.V. Likhanova, M.A. Domínguez-Aguilar, J.M. Hallen, L.S. Zamudio, E. Arce, Appl. Surf. Sci. 252 (2006) 2139–2152.
[42] F. Bentiss, M. Traisnel, L. Gengembre, M. Lagrenée, Appl. Surf. Sci. 161 (2000) 194–202.
[43] M. Mouanga, P. Berçot, J.Y. Rauch, Corros. Sci. 52 (2010) 3984–3992.
[44] K. Aramaki, Corros. Sci. 43 (2001) 1985–2000.
[45] K. Babić-Samardžija, C. Lupu, N. Hackerman, A.R. Barron, A. Luttge, Langmuir 21 (2005) 12187–12196.
[46] G.P. Lopez, D.G. Castner, B.D. Ratner, Surf. Interf. Anal. 17 (1991) 267–272.
[47] F. Moulder, W.F. Stickle, P.E. Sobol, K.D. Bomben, in: J. Chastain (Ed.), Handbook of X-Ray Photoelectron Spectroscopy, Perkin-Elmer Corp., Minnesota, USA, 1992.
[48] S. Manov, F. Noli, A.M. Lamazouere, L. Aries, J. Appl. Electrochem. 29 (1999) 995–1003.
[49] M. Royer, G. Herbette, V. Eparvier, J. Beauchêne, B. Thibaut, D. Stien, Phytochem. 71 (2010) 1708–1713.
[50] P. Bommersbach, C. Alemany-Dumont, J.P. Millet, B. Normand, Electrochim. Acta 51 (2005) 1076–1084.